

PRELIMINARY RESULTS OF THE BTF-105A TEST:
AN IN-REACTOR INSTRUMENT DEVELOPMENT AND FUEL BEHAVIOUR TEST

J.W. DeVAAL, J.D. IRISH, L.W. DICKSON, S.T. CRAIG,
M.G. JONCKHEERE AND L.R. BOURQUE

Fuel Safety Branch
Reactor Safety Research Division
AECL
Chalk River Laboratories
Chalk River, Ontario, Canada
K0J 1P0

ABSTRACT

The BTF-105A test, performed in 1996 March, was the first of a pair of in-reactor tests planned to investigate fuel behaviour and fission-product release from CANDU-type fuel for the high-temperature conditions expected following large-break loss-of-coolant accidents (LOCA) with coincident loss-of-emergency-core-cooling (LOECC). The BTF-105A test assembly consisted of an instrumented fuel stringer containing a single, unirradiated, fuel element; while the second test, denoted BTF-105B, will use a similarly instrumented assembly containing a single, previously irradiated, fuel element. As the first of these two tests, the primary objectives of BTF-105A were to test instrumentation and procedures planned for use in BTF-105B, and to obtain data on the relationship between fuel-centreline and sheath temperatures under transient conditions with steam cooling. This paper describes the conduct and preliminary results of the BTF-105A test, and also indicates improvements to be made for the upcoming BTF-105B test.

1.0 INTRODUCTION

The objective of the Blowdown Test Facility (BTF) experimental program is to obtain fuel behaviour, and fission-product release and transport data from in-reactor tests of CANDU-type fuel under representative accident conditions.^{1,2} Data from these tests are used in developing and validating computer codes³ used in the safety analysis and licensing of CANDU reactors.

The BTF is located in the NRU reactor at AECL's Chalk River Laboratories. As shown in Figure 1, instrumented fuel stringers are installed in the central channel of a reentrant test section, where they can be cooled by pressurized water or saturated steam provided by the U-1 loop. A test is initiated by isolating the test section from the U-1 loop cooling circuit and then opening the blowdown valve to depressurize the coolant through an instrumented blowdown line into a sealed blowdown tank. As the test section depressurizes, separate steam and/or inert gas purge systems are used to cool the fuel and to sweep fission products through the blowdown line. The blowdown line is instrumented to measure coolant thermalhydraulic parameters and, using an extensive collection of gamma spectrometers, fission-product gamma emissions. Steam and/or inert gas purge flows and the NRU reactor power level are controlled to obtain the target temperatures.

With the experience gained from the previous BTF-107^{4,5} and BTF-104⁶ tests, the BTF-105 experiment was divided in two to provide a separate test of instrumentation and procedures using an unirradiated fuel element (BTF-105A), before focusing on measuring fission-product releases from a previously irradiated fuel element (BTF-105B) at 1800-2000°C. This strategy, which also permitted the collection of fuel-centreline temperatures for validating fuel behaviour codes,³ was designed to increase the quality of fuel temperature measurements and to provide more assurance that the overall objectives of the BTF-105 experiment are met.

This paper describes the conduct and preliminary results of the BTF-105A test. Conclusions and recommendations are summarized, along with changes to instrumentation and test procedures designed to improve data quality and ensure a successful BTF-105B test.

2.0 THE BTF-105A TEST

A cross-section through the BTF-105A test assembly at the fuel element midplane is shown in Figure 2. The unirradiated 3.3% enriched, Bruce-geometry, fuel element was instrumented with two C-type fuel-centreline thermocouples, designated TFC01 and TFC02, located at the top bearing pad elevation and midway between the middle and bottom bearing pads, respectively. External fuel element instrumentation included three C-type, rhenium-clad thermocouples (TFS01, TFS02, and TFS03) attached with small Zircaloy clamps at the top, middle, and bottom bearing pads respectively (the TFS02 clamp can be seen in Figure 2); and three K-type, zirconium-clad thermocouples attached by laser welding at the top bearing pad elevation (TFS06), midway between the top and middle bearing pads (TFS04), and midway between the middle and bottom bearing pads (TFS05).

The fuel element was installed inside a multi-layered thermal shroud to protect the facility from the high fuel temperatures. The central flow tube in the shroud was made from NILCRA (100% TD[†] ZrO₂), and was instrumented with a combination of C and K-type thermocouples (designated TSTL01 - 06) installed in grooves in the outside of the NILCRA. The surrounding Zircaloy-clad shroud was filled with a lower-density ZIRCAR (21% TD[†] ZrO₂), which was back-filled with krypton to reduce thermal conductivity. The outside surface of the shroud was grooved to accommodate two longitudinally-wound hot spot detectors. Larger grooves on opposite sides of the shroud contained five outer wall thermocouples (designated TSTO01 - 05), and a self-powered rhodium flux detector (RR02).

Other components built into the fuel stringer were a pair of turbine flowmeters to measure flow over the fuel and a steam preheater located above the thermal shroud, and a NILCRA-lined debris retainer and an instrumented tube containing deposition coupons located below the thermal shroud. Evacuated chambers were mounted on the hanger bar to capture fission product samples from the gap sample tubes.

The most significant changes made to the facility were the addition of an aerosol sampling system, which draws samples from the blowdown line a few metres upstream of the sampling stations, and a cross-correlation flowmeter (also located just upstream of the sampling stations). Using a series of thermocouples at known positions along the centreline of a length of the blowdown line, the new flowmeter measures temperature perturbations within the coolant. Hence, by determining the time required for the perturbations to traverse the distance between thermocouples, a flow rate is calculated. Another facility change was the addition of separate trace heating to each sample line to prevent condensation in the sample lines, while sampling, and the resulting thermalhydraulic surging seen in the BTF-104 test.

2.1 Conduct of the Test and Observations

The test assembly was irradiated in pressurized water coolant at a linear power of about 50 kW/m for 10 days to establish an inventory of short-lived fission products. Following this irradiation, the stringer was subjected to a blowdown and a controlled high-temperature transient.

To simplify facility thermalhydraulic behaviour, the NRU reactor was shut down and the U-1 loop was converted to saturated steam cooling. The reactor was restarted, and a stepped startup was performed. At the completion of the startup in steam, reactor power was held at 55% demand power* for about 20 minutes, after which the power was quickly reduced to 2% demand prior to performing the blowdown. The blowdown was initiated and a steam purge flow was established as the test section depressurized. Inlet and outlet test section pressures (PIE12 and POE12, respectively) during the transient are shown in Figure 3. About a minute after blowdown, the signal from the remaining functional turbine flowmeter (FTM4) dropped to zero. (The FTM5 turbine had failed during the soak irradiation.) At this time, turbine failure was

[†] TD: Theoretical Density

* 85% demand power is full reactor power for NRU

assumed and it was decided to proceed with the test section inlet steam purge flow (FSPSH) set to a flow rate of ~ 10 g/s.

Figure 4 presents the response of fuel-centreline thermocouples TFC01 and TFC02, and the relative reactor neutron level (RRNL). A rapid drop in the centreline temperatures can be seen starting at 120 s, in response to the decrease to 2% demand power. The response of the fuel to the blowdown and subsequent power increases throughout the transient can be seen in the significant increases in the centreline temperatures and the development of a larger axial temperature gradient after the blowdown at 510.8 s.

The supplied steam and inert gas purge flows are shown in Figure 5. About five minutes after blowdown, the inert gas purge was activated to supply inert gas (0.1% H₂ in He) to the blowdown tank for hydrogen dilution purposes, and to confirm operation of the system for its use in post-test cooling. Liquid water from the gas supply line entered the test section, and resulted in the significant drop in fuel-centreline temperatures to less than 300°C from about 850 to 950 s in Figure 4. By 950 s the water was cleared from the supply line, and the inert gas purge flow was established at about 1.1 L/s. This gas flow was maintained for about another four minutes (until 1307 s) and then shut off until the end of the test, when it was re-established for post-test cooling. Figure 5 also shows that the steam purge flow decreased to about 7 to 8 g/s before the inert gas flow was shut off, and was maintained at this level for the remainder of the test.

As shown on the RRNL curve in Figure 4, reactor power was increased and held at plateaus of 3, 4, 8, 10, 13 and $\sim 15\%$ demand power during the transient. The final brief reduction to $\sim 12\%$ demand was in response to the outer wall temperatures of the thermal shroud approaching the reactor trip limit. It was noticed during the test that fuel temperatures sometimes declined significantly. The first time this happened, at about 1700 s, fuel temperatures dropped by about 200°C while the reactor power was constant at 3% demand. A more significant reduction occurred at about 2400 s, while the reactor power was being raised to 10% demand. The cause of these decreases in measured fuel temperature were later diagnosed to be the result of periods of higher steam flow through the test section (see Section 3.1).

Approximately 48 minutes into the test (at 2905 s), the target fuel-centreline temperature of 1900°C was reached. After about three minutes of operation within the target fuel temperature range (at about 3100 s) the thermal shroud failed. (Evidence of this failure was the rapid increase in the shroud internal pressure to the local coolant pressure.) Immediately following the shroud failure, a rapid increase in the outside shroud temperatures was observed. The outer shroud temperature adjacent to the bottom bearing pad of the fuel element (TSTO04) came within 100°C of the 875°C trip threshold; consequently, a power setback to 12% demand was requested.

Twenty seconds after the requested power setback, fuel, coolant, and shroud temperatures plunged suddenly. A few seconds later fuel failure was detected by the blowdown line gamma monitors (at 3177.3 s). The target fuel temperatures had been maintained for more than 4.5 minutes. Following the rapid drop in temperatures, fuel-centreline temperatures increased to a new steady-state value of 400 to 600°C. It became apparent that the increased cooling in the test

section, due to the presence of liquid water, would not be overcome easily, and the decision was made to activate the stringer grab samples and to switch the aerosol sampling system from its initial thimble filter to one of the cascade impactors before requesting a reactor shutdown.

After the test, it was hypothesized that the sudden drop in temperatures was the result of a build-up of condensed water at the bottom of the re-entrant test section which swept through the test section. Evidence of condensation running down the walls of the pressure tube and pooling at the entrance to the test section is seen in the drop to saturation temperature ($\sim 150^{\circ}\text{C}$) of the lowermost pressure tube thermocouple (TPT01) beginning at about 1500 s in Figure 3. It is also believed that the drop in power from 15 to 12% demand during a period when the test section pressure was unusually high ($> 1\text{ MPa}$) could have initiated the reflux of liquid through the test section by producing a situation where condensation briefly increased.

Post-test analyses focused on qualifying instrument performance and determining the fuel power and steam flow over the fuel during the transient (see Sections 2.2 and 3.1). Initial post-irradiation examinations focused on investigating the thermal shroud failure and determining the status of the turbine flowmeters (see Section 3.2).

2.2 Selected Instrument Performance

As can be seen in Figure 6, the fuel sheath thermocouples TFS01, TFS05 and TFS06 did not respond similarly to the other sheath thermocouples. This was first noted during the soak irradiation, where it was determined that the cladding of the TFS05 and TFS06 (K-type) thermocouples had failed (with subsequent water ingress causing the temperature offsets), and the electrical connections to the TFS01 (C-type) thermocouple had shorted in the top closure area during the first startup of the reactor. Data from the remaining sheath thermocouples were consistent with the fuel-centreline thermocouples, with the exception that the TFS04 thermocouple and the faulty TFS05 (K-type) thermocouple were driven off-scale during the highest-temperature period. The main instrumentation lessons learned were that K-type sheath thermocouples could not be expected to survive these high-temperature conditions, and that attaching spaded tip thermocouples by laser welding was prone to causing thermocouple cladding failures. The good performance of the remaining TFS02 and TFS03 (C-type) thermocouples attached with Zircaloy clamps has led to this technology being adopted for the BTF-105B test.

The overall performance of the thermocouples used behind the NILCRA liner was good, with no cladding failures observed during the soak irradiation. However, two of the three K-type thermocouples were driven off-scale during the highest-temperature period. As a result, it was recommended that K-type thermocouples not be used below the top bearing pad elevation in the BTF-105B test.

3.0 PRELIMINARY POST-TEST ANALYSES

Thermalhydraulic analyses and preliminary in-cell PIE have been performed. Detailed fission product release analysis has not yet been done. The low fission product releases and the flow fluctuations during BTF-105A reduced the value of data from the aerosol collection system.

Releases are expected to be much larger and steps will be taken to regulate the flow better during BTF-105B. This should lead to better performance of the aerosol system.

3.1 Fuel Power and Flow

The power history for the fuel element was determined from test assembly calorimetry under pressurized water cooling conditions coupled with neutron flux measurements from the RR02 flux detector. The power history for the water-soak irradiation (where power was assumed to be proportional to the RR02 measurement) and the ORIGEN computer code were utilized to estimate the γ and β sources for decay heat at the time chosen for normalizing to the RR02 readings. An MCNP transport calculation was used to assess the γ heating distribution within the test assembly components, where it was assumed that all of the β energy is deposited in the fuel. These MCNP transport calculations, and separate criticality calculations for water- and steam-cooled conditions, provided an estimate of how much the test element power increased relative to the rhodium flux detector reading when the cooling was changed from water to steam (1.08).

Decay heat within the fuel at every point during the irradiation was estimated using the DECAYHEAT computer code. This was combined with the above analyses to determine the total power (prompt plus decayed) and partition it to either the fuel plus sheath or coolant plus shroud. Figure 7 presents the results of the fuel power analyses for the test transient, showing the calculated powers deposited in the fuel and sheath, and coolant and shroud, respectively. Note that although higher temperatures were reached in BTF-105A than in BTF-104, the maximum fuel power was actually higher in BTF-104⁶ than in BTF-105A. This strongly suggested that the steam flow over the fuel was generally lower during the BTF-105A transient than during the BTF-104 transient.

The FTM5 flowmeter failed during the soak irradiation and flow through the FTM4 flowmeter fell below its stall limit (see Section 3.2). As a result the flow over the fuel was estimated from the flow into the blowdown tank (from blowdown tank level measurements) and the flow through the blowdown line cross-correlation flowmeter (CCFM). As seen in Figure 8, the integrated flow as measured by the CCFM and by blowdown tank mass gain are in better agreement with each other than they are with the integrated steam purge supply flow (FSPSH). CCFM data were updated on a 60 s interval, hence the comparatively slow response of this measurement. At about 1000 s after blowdown the flow into the blowdown tank, calculated by both methods, was about 2 kg more than supplied (because of the injection of water through the inert gas purge line), but then decreased significantly between 1000 and 3100 s due to condensation. These calculations also show a significant increase in the blowdown tank weight from 3200 to 3500 s, which represents the built-up condensate flushing through to the blowdown tank. Because the CCFM was designed to measure steam flow, condensed water could have passed undetected beneath the CCFM thermocouples, resulting in the observed 4 kg shortfall relative to the total mass-gain at the blowdown tank.

The flow rate into the tank, obtained by differentiating the blowdown tank level data is also provided in Figure 8. This curve shows that the test section flow rate was non-uniform, with periods of near-zero flow interspersed with periods of flow of up to a few grams per second. The

periods of higher flows correlate well with the observed periods of decreased fuel and sheath temperatures (see Figures 4 and 6, respectively). Flow data derived from the blowdown tank mass gain have been used in simulations of the test³.

3.2 Post-Irradiation Examination (PIE) of the Test Assembly

Immediately after the test, a gamma scan of the stringer inside its storage can was performed. This scan revealed that the low-volatile fission products associated with the fuel (e.g., La-140) were present almost exclusively at the original fuel location, indicating that the fuel pellet stack was largely intact. As a result of this finding, and recognizing that it would simplify examination of the instrumentation and the thermal shroud, the initial PIE of the fuel stringer was performed without first encasing it in epoxy.

The fuel stringer was cut into three pieces to isolate the fuelled section from sections containing the turbine flowmeters and deposition coupons. The two flowmeters were both found to be electrically functional. A calibrated nitrogen flow was passed through the assembly to examine the response of the two flowmeters. The upstream turbine (containing carbide bearings) was functional, while the downstream turbine (which contained alumina bearings) remained stalled. Further testing showed that the start and stall flow values of the upstream (FTM4) flowmeter were unchanged from its original calibration. It was concluded that the FTM4 flowmeter was fully functional during the test; but the steam flow fell below the turbine stall flow-rate and remained below the startup flow-rate throughout the transient. The flow-rate calculated from the blowdown tank mass gain and from the cross-correlation flow meter support this conclusion.

The shroud had no external damage (other than the development of a thin black oxide), and there was no evidence of creep deformation of the outer shroud wall. The debris retainer, when sectioned longitudinally, was free of any visible debris. Any debris that entered the retainer during the transient was probably smaller than the 3 mm holes in the retainer sieve plate and was simply swept through the retainer.

The thermal shroud was cut open longitudinally, and was opened by removing the upper half of the outer shroud wall with its enclosed low-density ZIRCAR still attached. The inner Zircaloy wall of the thermal shroud was found to be heavily oxidized and broken up in a 50 mm wide zone near the elevation of the lower bearing pad of the fuel element. Evidence of steam ingress into the ZIRCAR could also be seen in the mating half of the shroud. The ZIRCAR insulation was intact except for some minor spalling on its interior surface and a 3 mm wide through-wall crack that lined up with the zone of heaviest damage on the inner Zircaloy wall. It was concluded that the rapid injection of steam into the shroud following failure of the inner wall caused the through-wall crack in the ZIRCAR insulation. This crack then provided a path for the hot steam to heat the outer wall of the shroud directly, which in turn caused the rapid rise in temperature recorded by the TSTO04 thermocouple.

4.0 CONCLUSIONS AND RECOMMENDATIONS

The BTF appears to be susceptible to upstream condensation, leading to reduced flow over the fuel, and the build up of a pool of liquid which can unexpectedly flush through the test section.

Changes have been made to permit using a mixture of He and CO₂ in the annulus between the pressure tube and its surrounding liner tube. The use of a gas mixture should provide better control of pressure-tube temperatures and prevent the formation of condensation. As a further improvement, the steam condensate drain system (which was not used previously due to calibration problems) will be used during the BTF-105B test. To extend the lower limit of flow-rate measurement, improved turbine flowmeters will be used and a cross-correlation flow meter -- will measure the flow just above the fuel element.

Of the many lessons learned about instrument performance, the most important was that the high-temperature rhenium-clad thermocouples attached with Zircaloy clamps remained functional and stayed in contact with the sheath throughout the test. As a result, this technology will be used in the BTF-105B test.

While more fuel PIE work remains to be done, some preliminary conclusions are:

- 1) The fuel failure came much later and at higher temperatures in the BTF-105A test than in previous tests employing higher burnup fuel. It appears that low burnup CANDU fuel (where the internal gas pressure remains below the coolant pressure) is fairly robust and may not fail until the oxidized sheath is challenged by the thermal stresses associated with rewet.
- 2) Low burnup CANDU-type fuel quenched from high temperatures appears to remain in a coolable geometry. This finding, based on post-test gamma scans of the BTF-105A fuel element, suggests that, although the fuel may be relatively fragile when cold, it must retain significant mechanical strength during quenching.
- 3) Initial calculations show that the integral releases in the BTF-105A test were significantly lower than in BTF-104. The lack of a large inventory of fission products at the grain boundaries may contribute to lower releases from the fuel during heatup and quench. Therefore, models that track the location of fission products within the fuel are needed to be able to predict the differences in release under accident conditions between relatively fresh and higher burnup fuel.
- 4) Experimental data were acquired that are being used in the validation of computer codes used in the safety analysis and licensing of CANDU reactors³.

5.0 ACKNOWLEDGEMENTS

The authors acknowledge the financial support of the CANDU Owners Group, consisting of the Canadian nuclear utilities (Ontario Hydro, Hydro-Quebec and New Brunswick Power) and AECL. The authors would also like to thank the members of the BTF Technical Review and Advisory Committee for their input in planning the BTF-105A test, and the AECL personnel who assisted in performing the test. The efforts of R.T. Peplinskie in preparing the figures for this paper are also acknowledged.

REFERENCES

1. Fehrenbach, P.J., and Wood, J.C., "Description of the Blowdown Test Facility COG Program on In-Reactor Fission Product Release, Transport and Deposition Under Severe Accident Conditions", AECL Report AECL-9343, June (1987).
2. Walsworth, J.A., Zanatta, R.J., Dickson, L.W., Keller, N.A., MacDonald, R.D., Fehrenbach, P.J., and Wadsworth, S.L., "The Canadian In-Reactor Blowdown Test Facility (BTF) Program in Support of Reactor Safety", IAEA-SM-310/102, presented at the IAEA Symposium on Research Reactor Safety, Operations and Modifications, Chalk River, Ontario, October 23-27, (1989).
3. Middleton, P.B., Rock, R.C.K., and Wadsworth, S.L., "FACTAR 2.0 Code Validation", to be presented at the Fifth International Conference on CANDU Fuel, Toronto, Ontario, Canada, September 21-25, (1997).
4. MacDonald, R.D., DeVaal, J.W., Cox, D.S., Dickson, L.W., Jonckheere, M.G., Ferris, C.E., Keller, N.A., and Wadsworth, S.L., "An In-Reactor Loss-Of-Coolant Test with Flow Blockage and Rewet", presented at the International Topical Meeting on Thermal Reactor Safety, Portland Oregon, July (1991). Also issued as AECL Report AECL-10464, October (1991).
5. DeVaal, J.W., Popov, N.K., MacDonald, R.D., Dickson, L.W., Dutton, R.J., Cox, D.S., and Jonckheere, M.G., "Post-Test Simulations of BTF-107: An In-Reactor Loss-Of-Coolant Test with Flow Blockage and Rewet", presented at the Third International Conference on CANDU Fuel, Pembroke, Ontario, Canada, October 4-8 (1992). Also issued as AECL Report AECL-10758, March (1993).
6. Dickson, L.W., DeVaal, J.W., Irish, J.D., Elder, P.H., Jonckheere, M.G., and Yamazaki, A.R., "The BTF-104 Experiment: An In-Reactor Test of Fuel Behaviour, and Fission-Product Release and Transport Under LOCA/LOECC Conditions", presented at the Fourth International Conference on CANDU Fuel, Pembroke, Ontario, Canada, October 1-4, (1995).

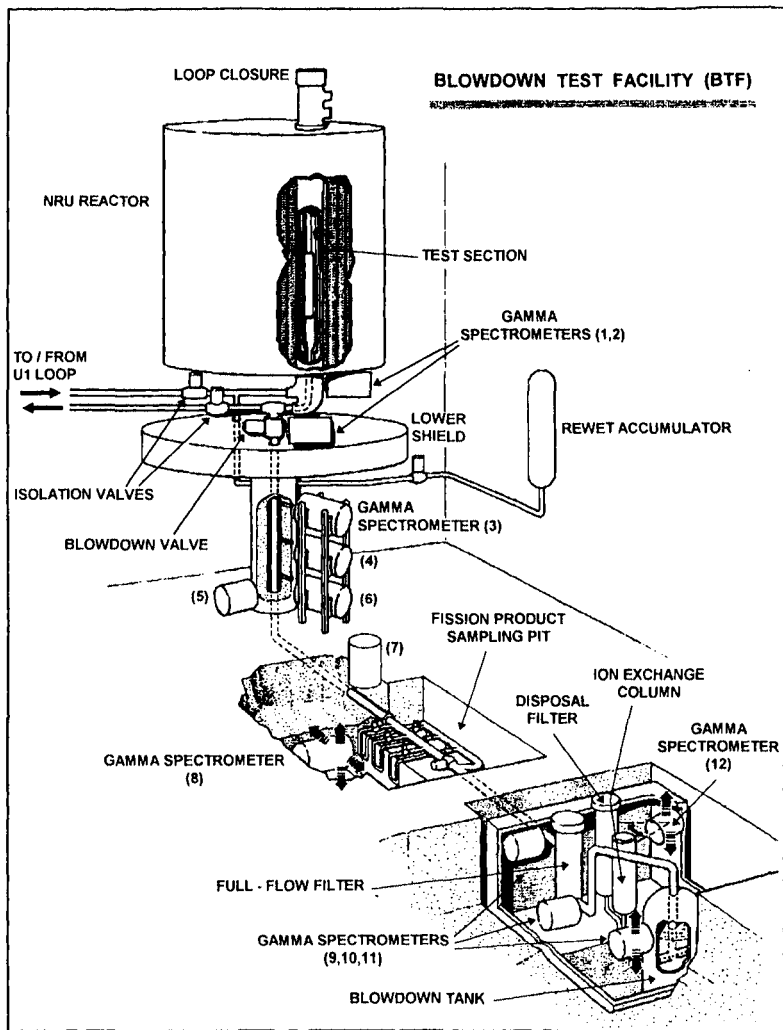


Figure 1: Schematic Drawing of the Blowdown Test Facility

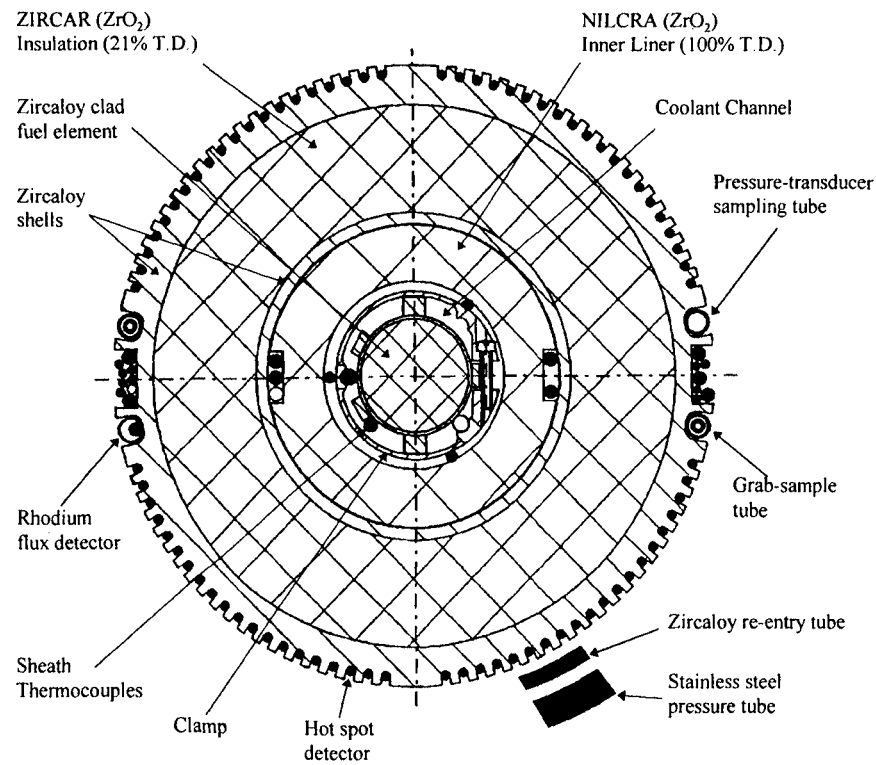


Figure 2: Cross-Section Through the BTF-105A Test Assembly at the Fuel Element Midplane

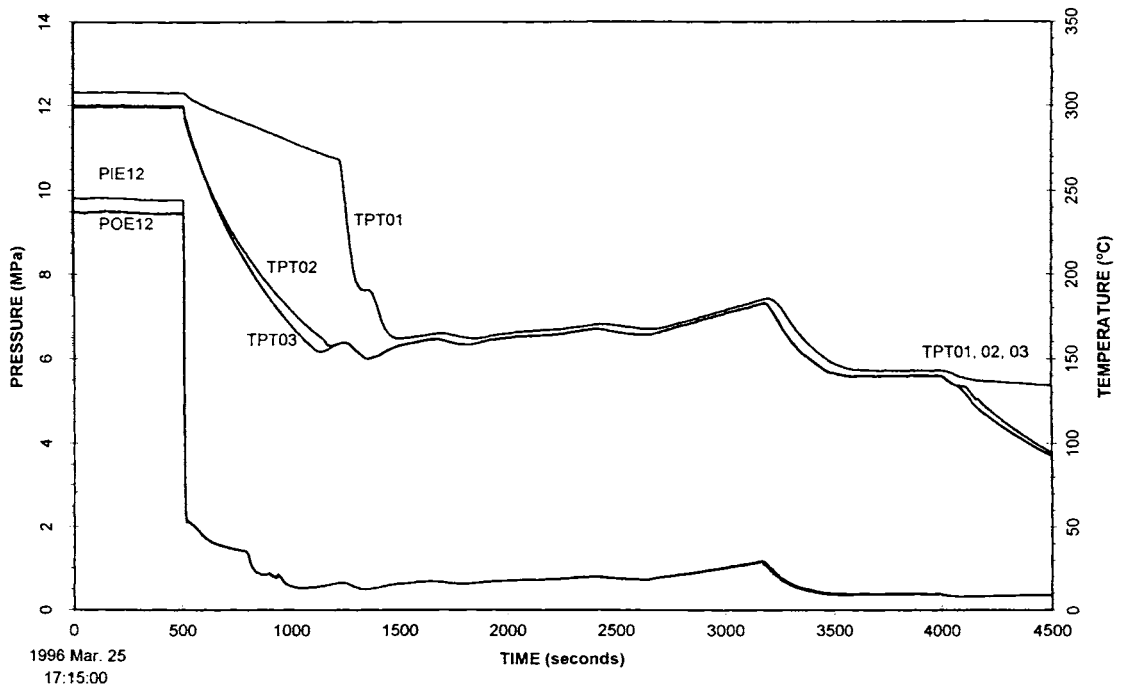


Figure 3: Measured Inlet (PIE12) and Outlet (POE12) Test Section Pressures and Pressure Tube Temperatures (TPT01, 02, 03) Below the NRU Core During Transient

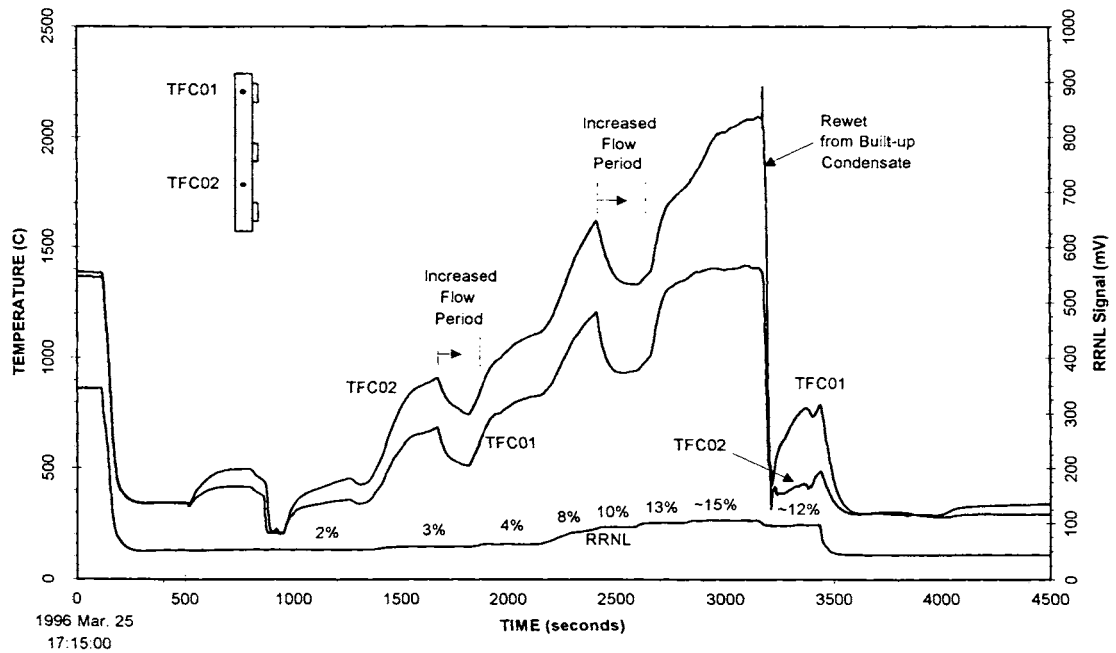


Figure 4: Fuel Centreline Temperatures (TFC01, TFC02) and NRU Neutron Level (RRNL)

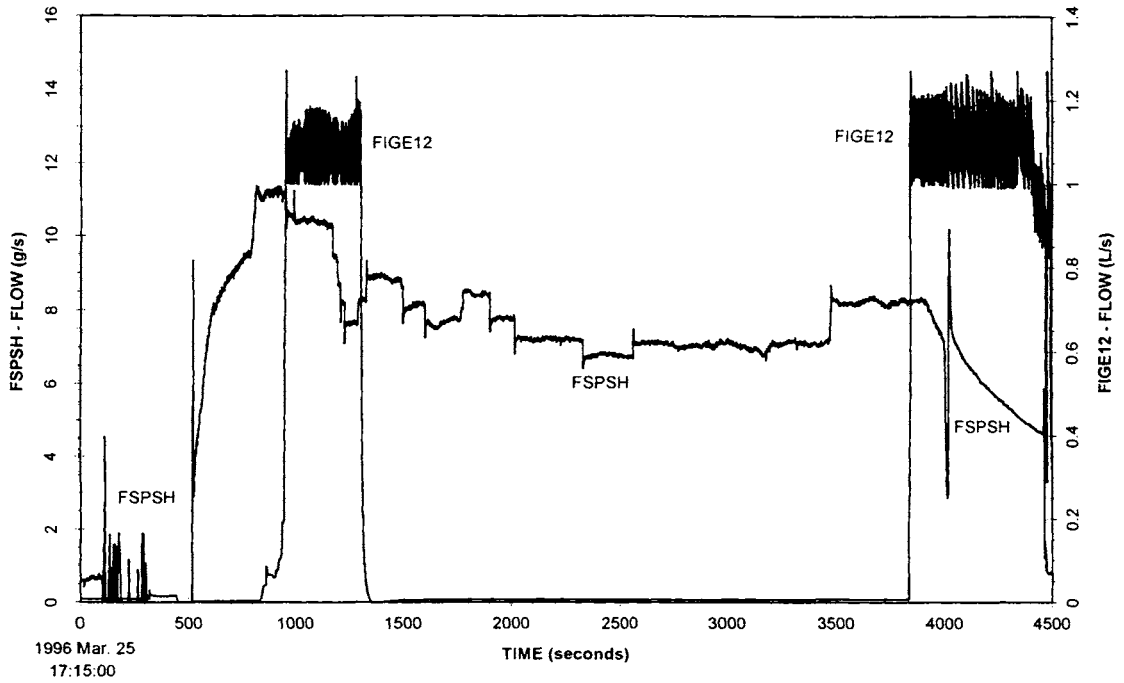


Figure 5: Steam Purge Supply Flow (FSPSH) and Inert Gas Purge Flow (FIGE12)

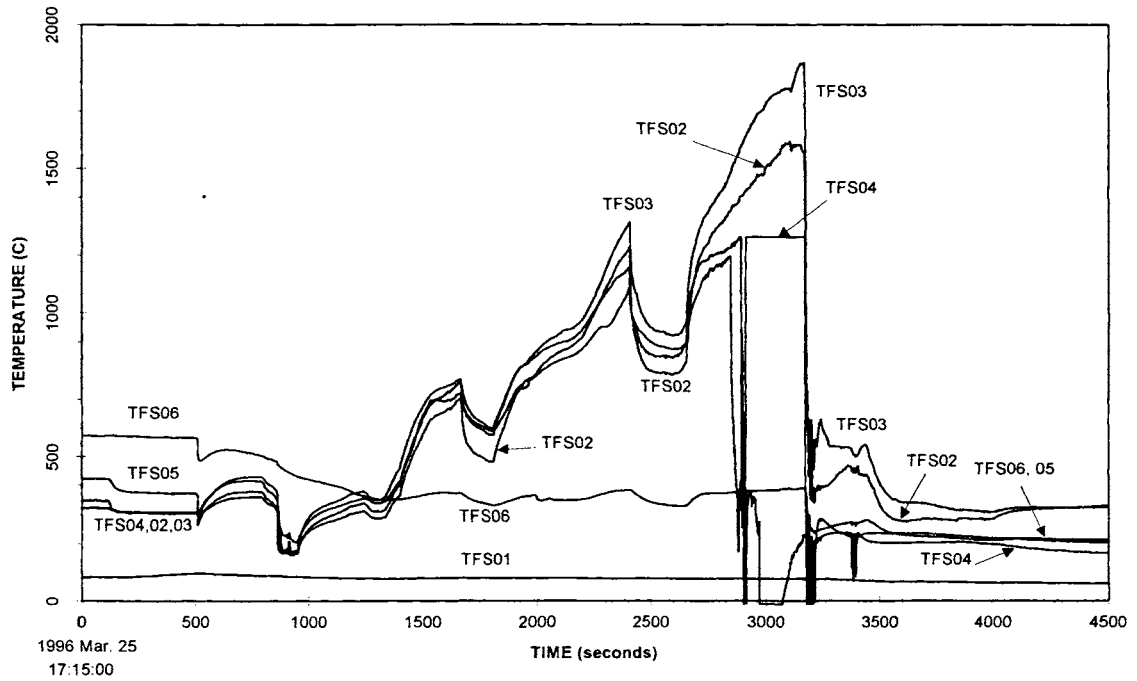


Figure 6: Fuel Sheath Temperatures (TFS01, 02, 03, 04, 05, 06) During Transient

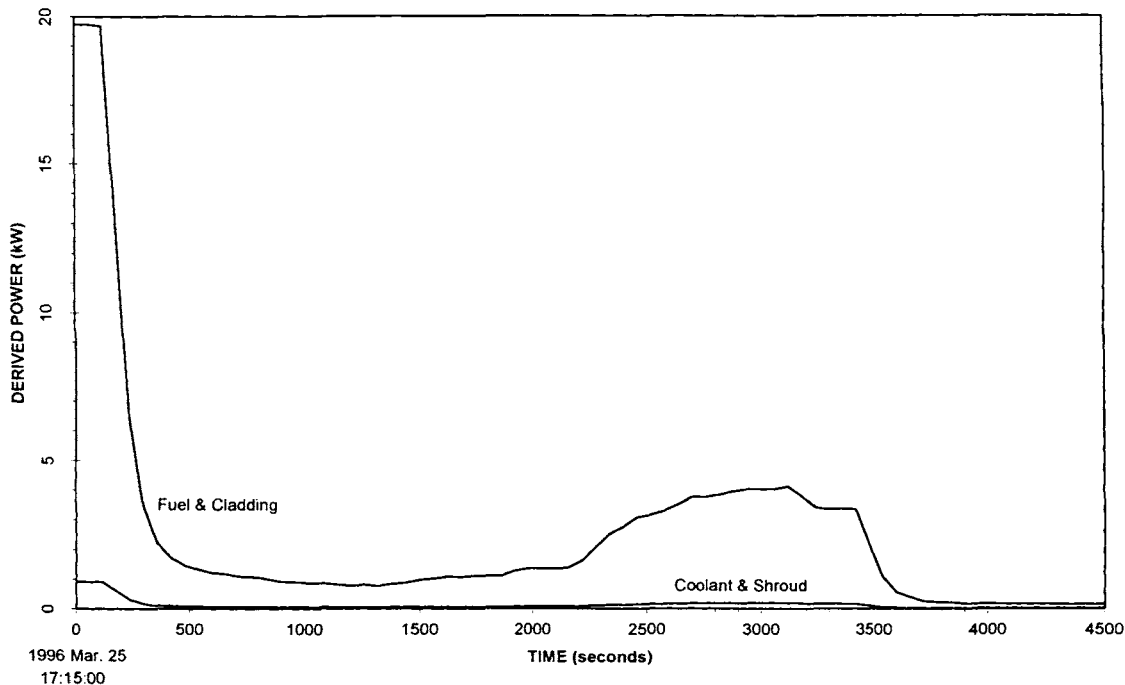


Figure 7: Calculated Power in Fuel & Cladding and Coolant & Shroud During the Transient

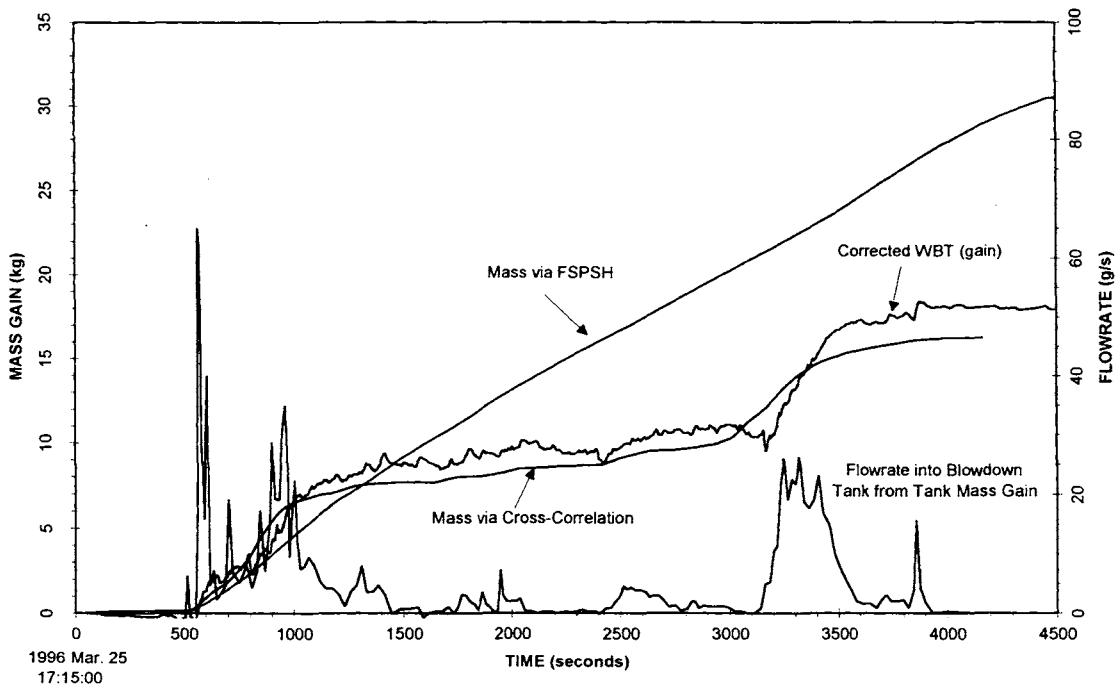


Figure 8: Integrated Steam Purge and Cross-Correlation Flows, Blowdown Tank Mass Gain, and Flow Rate into Blowdown Tank from Tank Mass Gain